

Evaluation of the Regenerative Effect of Rabbit BMMSCs and ADSCs. An In Vivo Study

Heba A. Shawky¹ and Dina M. Hassouna²

Abstract

Background: Bone marrow mesenchymal stem cells (BMMSCs) and Adipose tissue stem cells (ADSCs) demonstrated promising results in promoting the regeneration process of the periodontium including alveolar bone.

Aims: The aim of this study was to compare the regenerative capacity of BMMSCs and ADSCs in chitosan scaffolds implanted in rabbit femur bony defects.

Methods: Fifteen New Zealand rabbits were enrolled in this study. Four holes were drilled in each rabbit. The rabbits were divided into 3 groups, 5 rabbits each. Group A (Control group) received chitosan gel only. Group B received Rabbit-BMMSCs in chitosan gel while Group C received Rabbit-ADSCs in carrier gel. Rabbits were sacrificed after 8 weeks. Morphological assessment was accomplished using Scanning Electron Microscope (SEM). Energy Dispersive x-ray Analysis (EDXA) was used to analyze different inorganic and organic elements.

Results: SEM showed homogenous bony surface with complete bone healing in the ADSCs group. BMMSCs group showed delayed healing while the control group exhibited primary phase of bone healing. EDXA results of Magnesium and Phosphorus weight % were significantly higher in ADSCs group than BMMSCs and control groups. Calcium and Ca/P ratio weight % exhibited the highest significant results in BMMSCs group more than control and ADSCs. Nitrogen weight % displayed the highest significant results in BMMSCs then decreased in ADSCs and control group. Additionally, Carbon weight % showed increased significant results in control group when compared to BMMSCs and ADSCs.

Conclusion: Both ADSCs and BMMSCs treatments promoted more bone formation compared to chitosan alone. Besides, ADSCs yielded superior regenerative capacity compared to BMMSCs.

Keywords: ADSCs, BMMSCs, Bone defect, EDXA, SEM.

1 Associate Professor of Periodontics- Preventive Dental Sciences Department- College of Dentistry- Princess Nourah bint Abdulrahman University- KSA.

2 Lecturer of Oral Biology - Faculty of Dentistry Fayoum University – Egypt.

INTRODUCTION

Periodontitis is an immune-inflammatory disease characterized by destruction of the periodontal tissues resulting in tooth mobility and finally tooth loss.¹ The main purpose of periodontal regeneration is to reestablish the destructed alveolar bone, cementum, and periodontal ligament. Various regenerative remedies have been applied such as enamel matrix derivatives, membranes for guided tissue regeneration, and bone grafts.² These therapies have shown high efficiency in case of infra bony and furcation defects.³ Recently, tissue engineering, using stem cells proved to be a promising approach for periodontal regeneration.

Stem cells are undifferentiated mesenchymal cells that are capable to develop under stimulation into various cell types. Mesenchymal stem cells (MSCs) have been widely used in the field of periodontal regeneration. They can be harvested from dental or non-dental origin.⁴ Examples of MSCs of dental origin are stem cells from human exfoliated deciduous teeth, dental pulp stem cells, periodontal ligament stem cells, stem cells from apical papilla, and dental follicle precursor cells.⁵ Different stem cells of non-dental origin have been implicated in periodontal regeneration such as adipose-derived stem cells (ADSCs) and bone marrow stem cells (BMMSCs).⁶

The bone marrow was the initially identified source of MSCs. Human studies verified that BMMSCs are capable to differentiate into marrow stroma, adipocytes, cartilage, and bone.⁷ BMMSCs were proven to enhance the regeneration of alveolar bone, periodontal ligament, and cementum.⁸ *In vitro* cultures of rat BMMSCs showed that they have increased mineralization and a higher osteocalcin content which is a marker of late osteoblast differentiation.⁹

Subsequently, adipose tissue appeared as a substituting source of MSCs.¹⁰ They have a great differentiation capacity and are able to proliferate into adipogenic, myogenic, chondrogenic, and osteogenic cells according to the lineage-specific stimulating factors.¹¹ ADSCs can be simply harvested and encompass

a great number of stem cells significantly more than that from BMMSCs.¹² Thus, adipose tissue is recognized as one of the most prosperous sources of stem cells and hence, offers great chances for application in the field of regeneration.¹³

In order to regenerate the damaged tissue, the stem cells should be combined with biomaterial scaffolds. Different natural and synthetic biomaterials have been utilized as scaffolds for stem cells.¹⁴ Synthetic biomaterials include polymer-based and ceramic-based scaffolds. Natural biomaterials, on the other hand, comprise scaffolds made from purified proteins or polysaccharides or using decellularized extracellular matrix. Protein-based biomaterials comprise collagen, fibrin, silk, vitronectin, and fibronectin scaffolds.¹⁵ Whereas, polysaccharide-based biomaterials comprise agarose, hyaluronan, alginate, and chitosan.¹⁶ Chitosan consists of glucosamine units and is derived by the deacetylation of chitin. It is a common scaffold in tissue engineering where its characteristics can be controlled through different chemical cross-linking processes. It has been previously used in developing replacement bone and cartilage or treating spinal cord injury or for wound healing.^{17,18} In the current study we compared the regenerative capacity of BMMSCs and ADSCs incorporated in chitosan scaffolds and implanted in bony defects created in rabbit femurs.

MATERIAL AND METHODS

Animals:

Fifteen New Zealand white rabbits aging 6 months and weighing between 3.5 – 4.5 Kgs were utilized in this study. The experimental study was run in the animal house of Faculty of Medicine, Cairo-University. The protocol for the present was approved by Ein Shams Ethics Committee with the number FDASU-Rec R032101. All rabbits were kept under the same nutritional and environmental conditions in the experimental animal house with respect to the five freedoms of

animals under human care.¹⁹ During the study, all rabbits were kept in polypropylene cages, two rabbits in each cage with ad libitum access to water and normal diet. They were daily monitored by the veterinarian in the animal house for pain, injury or disease. The room temperature was about 22-24°C and the animals were exposed to 12:12 hours light dark cycles. The rabbit population was health observed according to commendations by Federation of European Laboratory Animal Science Associations (FELASA).²⁰ The rabbit population was divided into 3 groups, 5 rabbits each according to the 3Rs (Replacement, Reduction, Refinement) guiding the use of animals in research.²¹

Sample size Calculation:

The sample size was calculated based on the data of reference Rady et al.,²² that the maximum difference between the three groups mean is 1.08 and the estimated pooled standard deviation is 0.96. Assuming the alpha error 0.05 and power 0.8 a number of 17 cases per group is required adding 3 cases for anticipated missing data it results in 20 cases per group a total of 60 cases. The calculation is carried out by Minitab version-16 statistical package. Thus 15 New Zealand white rabbits were enough to carry the experiment as follows; 5 rabbits/group, 4 holes/ rabbit, 20 holes in each group.

Stem cell preparation:

The preparation of stem cells was held in Laboratory – Biochemistry Department – Cairo University. Rabbit BMMSCs preparation was performed according to Zhang et al.²³ while preparation of rabbit ADSCs was according to Semyari et al.²⁴

Anesthetic protocol:

Rabbits were anaesthetized using intramuscular injection of Xylazin (Chanelle pharmaceutical manufacturing Ltd., Ireland) 5 mg/kg body weight and Ketamine hydrochloride (Pfaffen-Schwabenheim, Germany) 30 mg/kg body weight.

Surgical protocol:

Surgical access to the right and left femur of each animal were performed with a linear 20 mm incision in the cranio-caudal direction, using a No. 24 scalpel blade. Then, the dissection of skin, muscle, and periosteum was performed to expose the bone surface. A rounded bur mounted on high-speed hand piece was used to drill 2 defects in each femur with at least 10 mm inter-distance (measured between the centers of the bone defects). The diameter of the bone defect was 6 mm and the depth was 10 mm. Drilling was performed under copious irrigation. Finally, the wound was sutured and the rabbit received analgesic (Cataflam 750 mg - the dose 10 mg/1kg) and antibiotic (Flumox 500 mg vial) after surgery. The drilled bone defects received different treatment modalities according to their assigned group as follows

- Group A (Control): A total of 20 holes (4 holes/rabbit, 2 holes in each femur) were injected with the chitosan carrier gel only
- Group B: A total of 20 holes (4 holes/rabbit, 2 holes in each femur) were injected in each with 1 million Rabbit-BMMSCs in carrier gel, where each hole was injected with 0.25 million Rabbit-BMMSCs.
- Group C: A total of 20 holes (4 holes/rabbit, 2 holes in each femur) were injected with 1 million Rabbit-ADSCs in carrier gel, where each hole was injected with 0.25 million Rabbit-ADSCs

Rabbit Sacrifice:

All rabbits were sacrificed after 8 weeks. They were sacrificed according to the AVMA euthanasia guidelines for common species used at Washington University²⁵ by injecting an over dose of a Pentobarbital (Diazepam, Roche, France) \geq 150 mg/kg body weight into an ear vein.

Assessments:

- 1- Scanning Electron Microscope (SEM): The assessment was performed to morphologically examine the newly formed bone in all groups. The specimens were fixed in 4 % formaldehyde with 1% glutaraldehyde. The specimens were rinsed in phosphate buffer for

10 minutes and then dehydrated by passing through series of 50%, 70% and 95% ethyl alcohol for 10 minutes each and then in absolute alcohol for two changes of one-hour period. After dehydration, the specimens were dried at the critical point and mounted using silver paint on the specimen holder then coated with gold through ion sputtering device.²⁶ After coating, the samples were examined by the Jeol scanning microscope (JSM-5300) in Faculty of Science, Alexandria University.

- 2- Energy Dispersive x-ray Analysis (EDXA): Mineral content of bony defects in different studied groups were examined by EDXA. The specimens were ground and polished using diamond paste to be (1µm size). Then, they were washed out under running water, dehydrated, and air-dried.²⁶ Surface of the bone was exposed to X-ray analysis using the EDXA system in Faculty of Science, Alexandria University.

Statistical analysis:

All Data were collected, tabulated and subjected to statistical analysis. Statistical analysis was performed by SPSS in general (version 20), while Microsoft office Excel was used for data handling and graphical presentation. Quantitative variables are described by the Mean, Standard Deviation (SD), the Range (Minimum – Maximum), Standard Error (SE) and 95% confidence interval of the mean. Shapiro- Wilk test of normality is used to test normality hypothesis of all quantitative variables for further choice of appropriate parametric and non-parametric tests. All the variables except one are found normally distributed allowing the use of parametric tests. One way analysis of variance ANOVA is used to compare the mean values of the three groups. Multiple comparisons were carried out by applying Bonferroni method. For the non-normally distributed variable Kruskal Wallis test is applied with Mann and Whitney U test for pair wise comparisons. Significance level is considered at $P < 0.05$ (S); while for $P < 0.01$ is considered highly significant(HS). Two Tailed tests are assumed

throughout the analysis for all statistical tests.

Results:

1. SEM Results:

a) Control (group A):

SEM revealed primary phase of bone healing in low and high magnification powers. Where, low magnification power for the whole surface of the bony defect showed newly bone filling the bony defect with incomplete fusion with old bone in most areas and minimum complete fusion in other areas as in (Fig. 1 – a). At the periphery, upon increasing magnification power showed, large area of granulation tissue filling the bony defect with very small area of bony trabeculae of newly formed bone and a well-defined space between the newly formed bone filling the bony defect and the old bone as in (Fig. 1 – b). While at the center with high magnification power, a large area of granulation tissue appeared filling the bony defect as in (Fig. 1 – c).

b) BMMSCs treatment (group B):

SEM showed delayed bone healing with high rate of bone remodeling showing areas of new bone formation and spaces of bone resorption in both low and high magnification powers. As low magnification power for the whole surface of the bony defect showed incomplete fusion between newly formed bone and old bone along the whole surface area of the bony defect at most areas. A small area of fusion between developing bone and old bone by dark grey area of granulation tissue appeared (Fig. 2 – a). At the periphery, upon increasing magnification power showed, large areas of bone trabeculae and bone marrow spaces filling the defect, a space with varying thickness, thin at some areas and thick in other areas. This space indicates incomplete fusion between the newly formed bone and old bone as in (Fig.2 – b). While at the center with high magnification power. It revealed areas of bone trabeculae and bone marrow spaces, large spaces, and areas of complete formation of bone with osteocytes lacunae on the outer bone surface as in (Fig. 2 – c).

c) ADSCs treatment (group C):

SEM displayed a completed bone healing surface in both low and high magnification powers. Hence, along the whole surface of bony defect in group (C) with low magnification power, showing homogenous bony surface with complete fusion of newly

formed bone and old bone (Fig. 3 – a). While at the periphery, complete fusion occurred between newly formed bone and old bone with line of demarcation separating them (Fig. 3 – b). Moreover, at the center of the defect, a homogenous newly formed bone appeared with similar architecture to old bone (Fig. 3 – c)

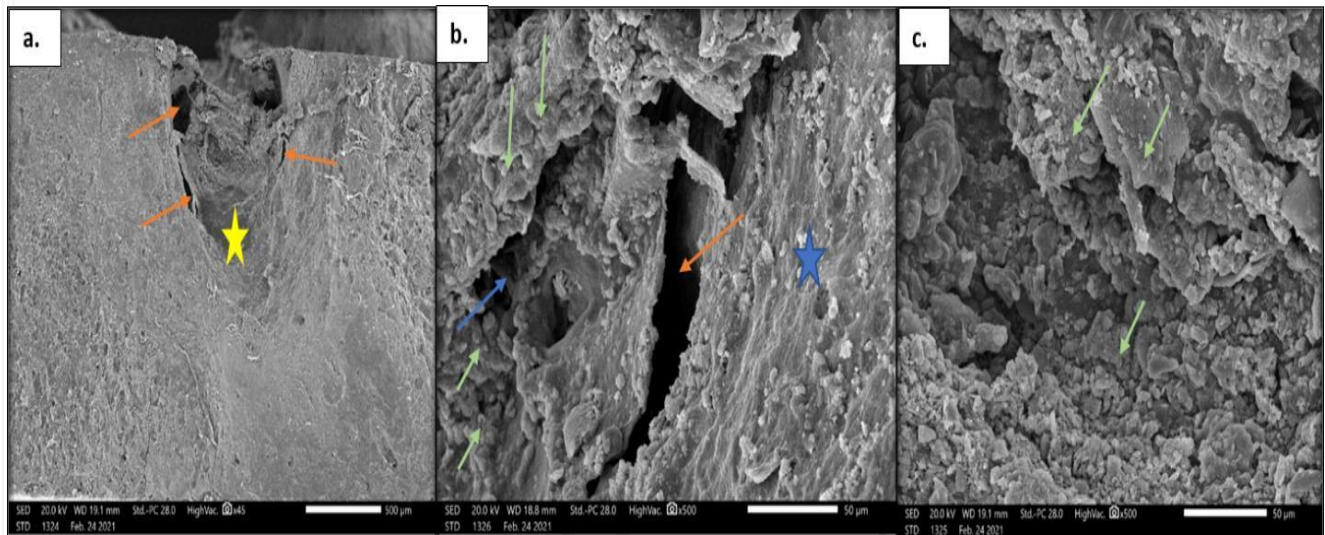


Fig. (1) Showing scanning electron micrograph of control group bony defect (A) with low magnification power (a), higher magnification at the periphery (b) and at the center (c). A wide space (orange arrow) was observed between the newly formed bone at the center and old formed bone (yellow astries) at the periphery. Small areas of newly formed bone trabeculae (blue arrows) were detected in the center with some granulation tissue (green arrows).

(a) (X45); (b & c) (X500)

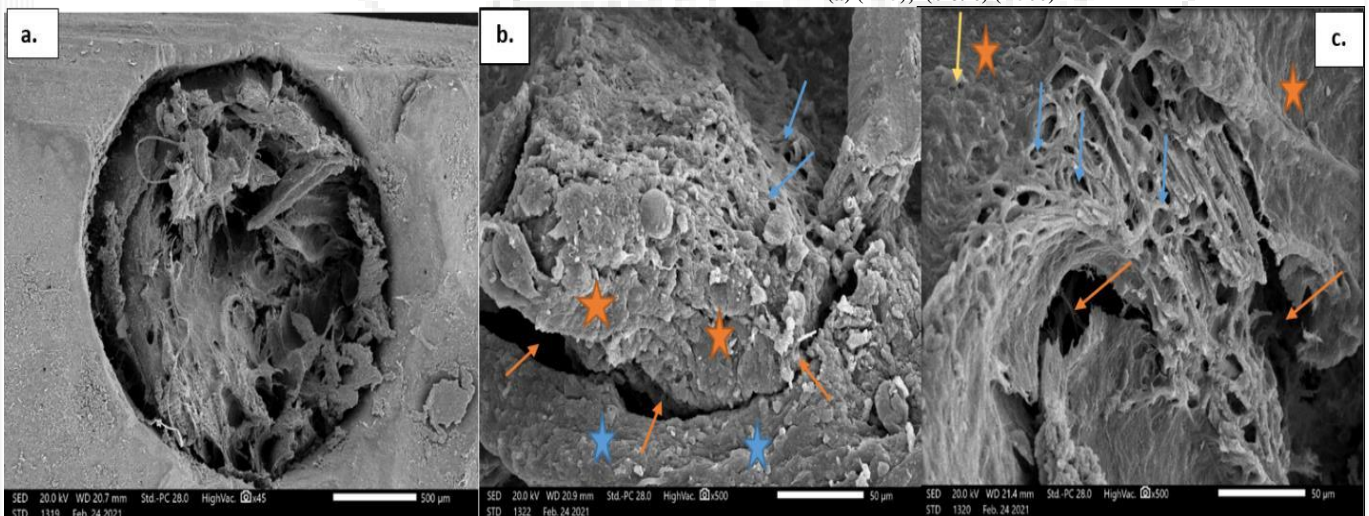


Fig. (2) Showing scanning electron micrograph of BMMSCs bony defect group (B) with low magnification power (a). Higher magnification at the periphery (b) and at the center (c). A wide space (orange arrow) was observed between the newly formed bone at the center (orange astries) and old formed bone (blue astries) at the periphery. Small areas of bone trabeculae and bone marrow spaces (blue arrows) were detected in the center. Large spaces between developing bones were also observed (orange arrows).

(a) (X45); (b & c) (X500)

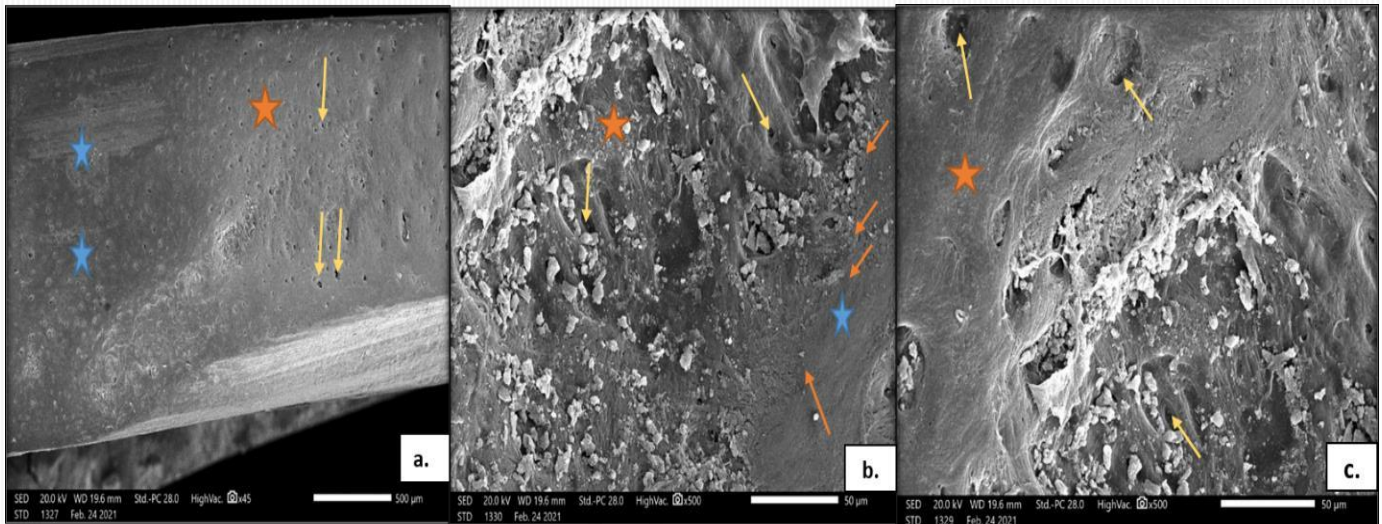


Fig. (3) Showing scanning electron micrograph of ADSCs bony defect group (c) with low magnification power (a). Higher magnification at the periphery (b) and at the center (c) with complete fusion between new bone (orange astries) and old bone (blue astries) with line of demarcation separating them (orange arrows), with osteocytes lacunae (yellow arrows) on the surface of newly formed bone (orange astries).

(a) (X45); (b & c) (X500)

2. EDXA Statistical Results:

The inorganic elements studied by EDXA were Calcium (Ca), Phosphorus (P), Ca/P ratio and Magnesium (Mg) weight %. While, the organic elements studied by EDXA were Carbon (C) and Nitrogen (N) weight %.

The inorganic elements, Ca and Ca/P ratio weight % results showed a statistically significant increase in BMMSCs group in comparison to the control group with the least results seen in ADSCs group. However, P and Mg weight % results showed the highest result

in ADSCs group with statistical significance then decreased in BMMSCs group followed by control group.

Regarding the organic elements, the highest results for C weight % occurred in control group then decreased in BMMSCs and ADSCs groups in descending order with statistical significance. Conversely, N weight %, BMMSCs showed the highest results with statistical significance followed by ADSCs and control group in descending order. The ANOVA statistical analysis results of the previous data are presented in table (1) and fig. (4).

Ain Shams Dental Journal

Table (1): Showing ANOVA statistical results of EDXA Results of inorganicelements, Ca, Ca/P ratio, P and Mg weight % and the organic elements C, N weight %

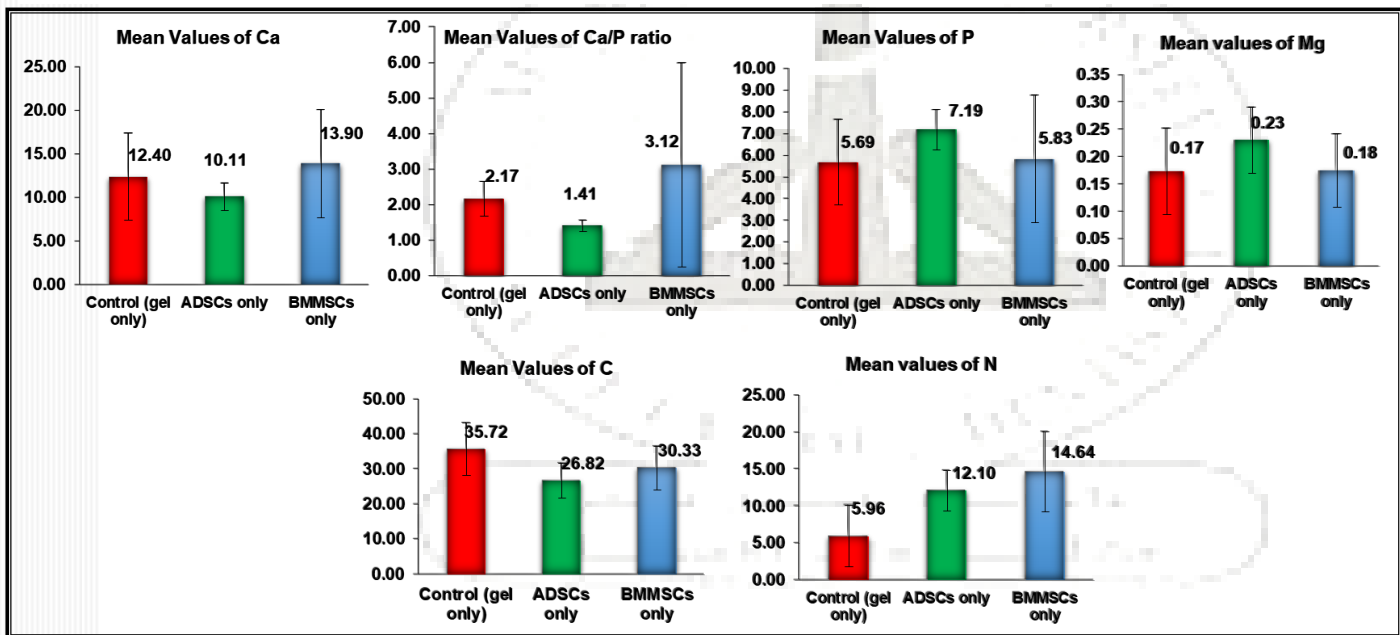
Ca %												
	N	Mean	SD	SEM	95% Confidence Interval for Mean		Minimum	Maximum	F	P Value		
					Lower Bound	Upper Bound						
Control (gel only)	20	12.40	5.00	1.12	10.06	14.74	4.00	22.00	3.28	0.04484	P < 0.05 S*	
ADSCs only	20	10.11	1.56	0.35	9.38	10.85	7.10	12.32				
BMMSCs only	20	13.90	6.24	1.39	10.98	16.81	2.60	20.17				
Ca/P ratio												
Control (gel only)	20	2.17	0.49	0.11	1.94	2.40	1.58	3.06	5.19	0.00852	P < 0.01 HS**	
ADSCs only	20	1.41	0.15	0.03	1.34	1.48	0.99	1.64				
BMMSCs only	20	3.12	2.88	0.64	1.78	4.47	0.57	12.71				
P%												
Control (gel only)	20	5.69	1.99	0.44	4.76	6.62	2.33	9.00	3.06	0.05478	P ≈ 0.05 Almost S*	
ADSCs only	20	7.19	0.93	0.21	6.76	7.62	4.87	8.30				
BMMSCs only	20	5.83	2.94	0.66	4.46	7.21	1.47	11.49				
Mg%												
Control (gel only)	20	0.17	0.08	0.02	0.14	0.21	0.00	0.29	4.36	0.01724	P < 0.05 S*	
ADSCs only	20	0.23	0.06	0.01	0.20	0.26	0.13	0.33				
BMMSCs only	20	0.18	0.07	0.02	0.14	0.21	0.07	0.30				
C%												
Control (gel only)	20	35.72	7.45	1.67	32.23	39.21	26.00	54.30	10.11	0.00017	P < 0.001** HS	
ADSCs only	20	26.82	4.96	1.11	24.50	29.14	8.00	31.63				
BMMSCs only	20	30.33	6.25	1.40	27.40	33.26	17.77	36.30				

N %												
Control (gel only)	20	5.96	4.14	0.92	4.02	7.90	0.00	13.00	22.22	0.00000	P < 0.001** HS	
ADSCs only	20	12.10	2.74	0.61	10.82	13.38	7.67	19.49				
BMMSCs only	20	14.64	5.40	1.21	12.11	17.17	4.07	19.27				

* Significant (S), P Value < 0.05

**High significant (HS) P value < 0.001

Fig. (4): Showing graph of mean values of EDXA Results of inorganic elements (Ca, Ca/P ratio, P, Mg) and organic elements (C, N) weight % respectively.



ASDJ
Arabian Science Dental Journal

Discussion:

The ultimate goal of periodontal tissue engineering is to reestablish both the architecture and function of the damaged periodontal tissue. Various types of stem cells were utilized in association with appropriate scaffolds to accomplish this goal. In the current study, we compared the regenerative capacity of both BMMSCs and ADSCs incorporated in chitosan scaffold and implanted in bone defects created in rabbit femurs.

Chitosan was selected to be used as a scaffold in the present study due to its ability to promote bone healing.²⁷ Former studies recognized that chitosan alone can enhance the differentiation of stem cells into osteoblasts and to augment bone growth.^{28,29} Subsequent studies proposed that the addition of osteogenic, osteoinductive and/or osteoconductive biomaterials to chitosan can further potentiate the bone regeneration procedure.^{30,31}

All animals were sacrificed after 8 weeks, and were examined using SEM. The control group which was implanted with Chitosan alone showed incomplete fusion between new and old bone in most of areas, while in BMMSCs group a small area of fusion between developing bone and old bone was detected. Better healing was observed in BMMSCs where large areas of bone trabeculae and bone marrow spaces were detected at sites of new bone formation. The large spaces occurred between new bone trabeculae formed in BMMSCs group in figure (2-a, b and c) could be interpreted to be areas of resorption during bone remodeling. These findings agree with Yang et al.³² who demonstrated better regenerative capacity with greater bone formation in rats' periodontal defects transplanted with BMMSCs. This was confirmed by Zang et al.³³ who presented that BMMSCs encourage greater bone formation in fenestration and Grade II furcation defects.

On the other hand, in ADSCs group;

SEM showed homogenous bony surface with complete fusion of newly formed bone formed and old bone. These findings were in convenience with Lemaitre et al.³⁴ who verified that grafting periodontal defects with ADSCs promotes the periodontal vascularization. Moreover, Hung et al.³⁵ confirmed that rabbit ADSCs exhibit advanced growth rate in culture and effectively promote alveolar bone regeneration when placed in extraction sockets of rabbit model. Accordingly, SEM results of the current study showed better healing outcome in ADSCs group compared to the BMMSCs group. These results confirm those of Walmsley et al.³⁶ who confirmed that ADSCs upgraded the rates of bone regeneration more than BMMSCs. The authors attributed the superior regenerative capacity of ADSCs to its exhibition of both increased survival and increased expression of collagen type I alpha 1 in comparison to BMMSCs.

We confirmed our SEM detections in the existing study with EDXA. EDXA is a supportive tool to analyze the constitution of mineralized tissues and the degree of bone mineralization by calculating the ratios of elements (atomic or weight).³⁷ Bone is a mineralized tissue formed of 60% inorganic constituent (hydroxyapatite crystals), 10% water, and 30% organic constituent (proteins).³⁸ In our study, the weight % of Ca, P, Mg and Ca/P ratio (from the inorganic bone components), and C, N content (from organic components) were detected.

In the current study, there was a significant decrease in Ca weight % and Ca/P ratio in ADSCs compared to control and BMMSCs. This could be related to that the finally repaired bone after healing is lamellar bone which has been fully mineralized, thus the porosity is less and the accumulated Ca ions were less as they had been incorporated in the hydroxyapatite crystals which further propagated mineralization.³⁹ In addition, the Mg weight % showed a significant increase in the

ADSCs group. Mg weight % plays a crucial role in the regulation of bone mineralization during remodeling.⁴⁰ Therefore, it is assumed that its increase inhibits mineralization manifested by the least amount of Ca detected in ADSCs group.

However, in the control group, the primary formed bone during healing is woven bone. This type of bone possesses an excessive amount of interfibrillar space that is occupied by mineral crystals and acidic proteins,⁴¹ which explains the increased amount of Ca and Ca/P ratio in such group.

The interpretation of the increased Ca and Ca/P ratio weight % in BMMSCs when compared to the control group is that, the woven bone had been replaced by trabecular bone as shown in SEM results indicating a high rate of bone remodeling at this site. Whereas, during demineralization phase of bone remodeling osteoclasts eliminate calcium ions.⁴² Thus, Ca will be accumulated at bone resorption site leading to an additional increase in Ca and Ca/P ratio levels. Besides; during bone formation phase of bone remodeling, mitochondria in osteoblasts play an essential indirect role in the process of mineralization by storing calcium and phosphate in the form of amorphous calcium phosphate.⁴³ Moreover, Calcitonin is released when blood calcium levels increase.⁴⁴ It inhibits bone resorption and promotes calcium salt deposition in bone matrix inhibiting osteoclasts thus increasing Ca and Ca/P levels.⁴⁵

Concerning the findings of Ca/P ratio, Liu et al.⁴⁶ inspected the impact of different Ca/P ratio on osteoblast viability, collagen formation, and activity of alkaline phosphatase. The study displayed that Ca/P ratios between 1 and 2 boosted the viability of osteoblasts and improved the activity of alkaline phosphatase. Accordingly, in the present study the Ca/P ratio of ADSCs group is 1.41 which optimizes the osteoblastic viability. On the other hand, the Ca/P ratio of

BMMSCs group in this study showed the highest value (3.13) indicating an increased action of bone remodeling especially bone removal by osteoclasts at bone healing site.⁴⁷

In the existing study, P weight % showed higher levels in ADSCs, then BMMSCs group compared to the control group. These results agreed with Rady et al.,²² who revealed a significant increase in the mean P weight % in the BMMSC-treated group relative to the PRF-treated group and concluded that BMMSCs promoted more adequate healing. The highest results for P weight % in this study were encountered in ADSCs group which points to that BMMSCs group yielded delayed bone healing compared to ADSCs group.

Mg is the second element in bone after Ca where 50% to 60% of body Mg is located within bone. Mg forms a surface constituent of the hydroxyapatite (calcium phosphate) mineral component. It is supposed to control and regulate the precipitation of calcium phosphate in the matrix of collagen of the bone.⁴⁸ In the current study, the highest Mg weight % was noticed in ADSCs group which could be related to the saturation of Ca and P ions, thus; reflecting complete saturation and healing in ADSCs. Therefore, it confirms the homogeneity of surface bone and the complete fusion of newly formed bone and old bone detected by SEM in ADSCs group.

The 30% organic constituent (proteins) of bone extracellular matrix consists of collagen type I (90 %) and non-collagenous proteins (10%).⁴⁹ Alterations of the relative proportions of these components were observed with age, site, gender, disease, and treatment.⁵⁰ Type I collagen is a triple-helical molecule including three polypeptide chains, each is composed of approximately 1000 amino acids.⁵¹ Chemically, an amino acid is a molecule that possesses a carboxylic (COOH) acid group and an amine group (NH₂), each is attached to a carbon atom called the α carbon. Thus, Nitrogen and Carbon are related to the major protein of bone collagen and can therefore be used as an indicator of the collagen content of bone.⁵²

In our study the lowest C weight percentage was encountered in ADSCs group followed by BMMSCs and control groups respectively. This can be attributed to fullmaturation of newly formed bone of ADSCs group. These results are in concurrence with Okata et al.⁵³ who suggested that C concentration decreases during calcification procedure whereas Ca and P increase. Similarly, Henmi et al.⁵⁴ determined that during the propagation of mineralization the Ca/P ratio increases and the proteins of the bone matrix measured in the form of C/Ca and C/P ratios reduces.

Regarding N weight %, the highest results in the present study were encountered in BMMSCs then ADSCs and the least results in control group. This could be related to increased bone remodeling in BMMSCs group compared to the control group. Whereas, the increased N weight % is related to Nitrogen-linked glycoproteins (N-Linked glycoproteins) which are components of non-collagenous proteins in bone

extracellular matrix which possess a significant role in bone remodeling and bone mineralization.⁵⁵ Bone sialoprotein (BSP) and osteopontin (OPN) are members of N-Linked glycoproteins of non-collagenous proteins in bone extracellular matrix.⁵⁶ BSP is expressed at the commencement of bone mineralization. It contains an N-terminal collagen-binding domain which facilitates binding of BSP to collagen which in turn enhances hydroxyapatite nucleation⁵⁷ which explains the elevated N weight % in fully mineralized ADSCs group. The highest level of N weight % detected in BMMSCs could be related to increased expression of both BSP and OPN. Where, Gordon et. al.⁵⁸ established that BSP augments osteoblast differentiation and matrix mineralization and OPN plays a significant role in bone remodeling.⁵⁹

The role of EDXA elements during bone formation were correlated to the results of the present study in table (2).

Table (2): Discussion summary of EDXA inorganic (Ca, Ca/P ratio, P & Mg) and organic elements (C & N) weight %.

Element (weight %)	Role during bone formation	Results	Interpretation
Ca	- Demineralized ions released from inorganic bone matrix during bone resorption phase during bone remodeling. ⁴³	BMMSCs > Control > ADSCs.	- Thus, increased Ca weight % is related to increased rate of bone remodeling in BMMSCs group confirmed by SEM results (Fig. 2).
Ca/P ratio	- Ca/P ratios between 1 and 2 increased the viability of osteoblasts and improved the activity of alkaline phosphatase. ⁴⁷	BMMSCs (3.13) > Control (2.17) > ADSCs (1.41).	- Thus, Ca/P ratio weight % of ADSCS group is 1.41 which optimize the osteoblastic viability.
P	- Enzymatic activity of alkaline phosphatase is required to generate enough of the free P mineral during bone mineralization. ⁶⁰	ADSCs > BMMSCs > Control.	- Thus, P weight % of ADSCS group indicated its full bone maturation confirmed by SEM results (Fig. 3)

Mg	<ul style="list-style-type: none"> - Plays a crucial role in the regulation of bone mineralization during remodeling.⁴⁰ - Control and regulate the precipitation of calcium phosphate in the matrix of collagen of the bone.⁴⁸ 	ADSCs > BMMSCs > Control.	<ul style="list-style-type: none"> - Therefore, it is assumed that Mg increase inhibits mineralization manifested by the least amount of Ca with the best SEM healing results detected in ADSCs group (Fig. 3).
C	<ul style="list-style-type: none"> - C is related to collagen protein found in bone.⁵² 	Control > BMMSCs > ADSCs	The least results of C observed in ADSCs group could be correlated to the least organic content with full maturation of newly formed bone (Fig. 3).
N	<ul style="list-style-type: none"> - N is to collagen protein found in bone.⁵² - N is also related to bone non-collagenous N-Linked glycoproteins (BSP & OPN) which possess a significant role in bone remodeling and bone mineralization.^{55, 56} 	BMMSCs > ADSCs > Control	<ul style="list-style-type: none"> - Increased N weight % in BMMSCs could be attributed to increased level of bone remodeling confirmed by SEM results (Fig. 2).

Conclusion:

SEM and EDXA element content results of ADSCs group showed superior bone healing followed by BMMSCs. Control group showed early phase of bone healing results.

References:

1. Graziani F. Nonsurgical and surgical treatment of periodontitis: how many options for one disease? *Periodontol* 2000. 2017; 75(1): 152–188.
2. Lin Z, Rios H.F, Cochran D.L. Emerging regenerative approaches for periodontal reconstruction: a systematic review from the AAP Regeneration Workshop. *J. Periodontol*. 2015; 86(2 Suppl): S134–S152.
3. Avila-Ortiz G, De Buitrago JG, Reddy MS. Periodontal regeneration - furcation defects: a systematic review from the AAP Regeneration Workshop. *J Periodontol* 2015; 86: S108-30.
4. Kobolak J, Dinnyes A, Memic A, Khademhosseini A, Mobasheri A. Mesenchymal stem cells: identification, phenotypic characterization, biological properties and potential for regenerative medicine through biomaterial micro-engineering of their niche. *Methods* 2016; 99: 62-68.
5. Bakopoulou A, Huang GT, Rouabhia M, Geurtsen W, About I. Advances and New Technologies towards Clinical Application of Oral Stem Cells and Their Secretome. *Stem Cells Int*. 2017; 2017: 6367375.
6. Hernández-Monjaraz B, Santiago-Osorio E, Monroy-García A, Ledesma- Martínez E, Mendoza-Núñez VM. Mesenchymal Stem Cells of Dental Origin for Inducing Tissue Regeneration in Periodontitis: A Mini-Review. *Int J Mol Sci*. 2018; 19(4): 944.
7. Lee C. C., Christensen J. E., Yoder M. C., Tarantal A. F. Clonal analysis and hierarchy of human bone marrow mesenchymal stem and progenitor cells. *Experimental Hematology*. 2010; 38(1): 46–54.
8. Du J, Shan Z, Ma P, Wang S, Fan Z. Allogeneic bone marrow mesenchymal stem cell transplantation for periodontal regeneration. *J Dent Res*. 2014; 93(2): 183-188.
9. Ito T, Sawada R, Fujiwara Y, Tsuchiya T. FGF-2 increases osteogenic and chondrogenic differentiation potentials of human mesenchymal stem cells by inactivation of TGF-beta signaling. *Cytotechnology*. 2008; 56 (1):1-7.
10. Zuk PA, Zhu M, Mizuno H, Huang J, Futrell JW, Katz AJ, Benhaim P, Lorenz HP, Hedrick MH. Multilineage cells from human adipose tissue: implications for cell-based therapies. *Tissue Eng*. 2001; 7(2): 211-228.

11. Paduano F, Marrelli M, Amantea M, Rengo C, Rengo S, Goldberg M, Spagnuolo G, Tatullo M. Adipose Tissue as a Strategic Source of Mesenchymal Stem Cells in Bone Regeneration: A Topical Review on the Most Promising Craniomaxillofacial Applications. *Int J Mol Sci.* 2017; 18(10): 2140.
12. Fraser J. K., Zhu M., Wulur I., Alfonso Z. *Methods in Molecular Biology.* Totowa, NJ: Humana Press; 2008; Adipose-derived stem cells: 59–67.
13. Ciuffi S, Zonefrati R, Brandi ML. Adipose stem cells for bone tissue repair. *Clin Cases Miner Bone Metab.* 2017;14(2): 217-226.
14. Williams DF. *Definitions in Biomaterials: Proceeding of a Consensus Conference of the European Society of Biomaterials,* Chester, England, March 3-5, Elsevier, Amsterdam. 1987.
15. Willerth, Stephanie M. and Sakiyama-Elbert, Shelly E. Combining Stem Cells and Biomaterial Scaffolds for Constructing Tissues and Cell Delivery. *Stem Journal.* 2019; 1(1): 1-25.
16. Diekjürgen D, Grainger DW. Polysaccharide matrices used in 3D in vitro cell culture systems. *Biomaterials.* 2017; 141: 96–115.
17. LogithKumar R, KeshavNarayan A, Dhivya S, Chawla A, Saravanan S, Selvamurugan N. A review of chitosan and its derivatives in bone tissue engineering. *Carbohydrate Polymers.* 2016; 151: 172–188.
18. Tao SC, Guo SC, Li M, Ke QF, Guo YP, Zhang CQ. Chitosan Wound Dressings Incorporating Exosomes Derived from MicroRNA-126-Overexpressing Synovium Mesenchymal Stem Cells Provide Sustained Release of Exosomes and Heal Full-Thickness Skin Defects in a Diabetic Rat Model. *Stem Cells Translational Medicine.* 2017; 6: 736–47.
19. Mellor DJ. Moving beyond the "Five Freedoms" by Updating the "Five Provisions" and Introducing Aligned "Animal Welfare Aims". *Animals (Basel).* 2016; 6(10): 59.
20. Reh binder C, Baneux P, Forbes D, van Herck H, Nicklas W, Rugaya Z, Winkler G. FELASA recommendations for the health monitoring of mouse, rat, hamster, gerbil, guinea pig and rabbit experimental units. Report of the Federation of European Laboratory Animal Science Associations (FELASA) Working Group on Animal Health accepted by the FELASA Board of Management, November 1995. *Lab Anim.* 1996; 30(3): 193-208.
21. Singh J. The national centre for the replacement, refinement, and reduction of animals in research. *J Pharmacol Pharmacother* 2012; 3: 87-89.
22. Rady, D, Mubarak, R, & Moneim, RAA. Healing capacity of bone marrow mesenchymal stem cells versus platelet-rich fibrin in tibial bone defects of albino rats: an in vivo study. *F1000Research.* 2018, 7.
23. Zhang W, Zhang F, Shi H, Tan R, Han S, Ye G, Pan S, Sun F, Liu X. Comparisons of rabbit bone marrow mesenchymal stem cell isolation and culture methods in vitro. *PLoS One.* 2014, 18; 9 (2): e88794.
24. Semyari H, Rajipour M, Bastami F, Semyari H. Isolation and culture of mesenchymal stem cells from rabbit scapular subcutaneous adipose tissue and their ability to differentiate into osteoblasts. *Avicenna Journal of Dental Research.* 2015;7(2): e22308.
25. American Veterinary Medical Association (AVMA) Guidelines for the Euthanasia of Animals:2020Edition.Available online: <https://www.avma.org/sites/default/files/2020-01/2020-Euthanasia-Final-1-17-20.pdf>
26. Eric L, Charles E, Patrick E, David C, Dale E. *Scanning electron Microscopy and x-ray microanalysis.* 3rd ed. USA: Klumer Academic Plenum publisher; 2003.
27. Venkatesan J, Vinodhini PA, Sudha PN, Kim SK. Chitin and chitosan composites for bone tissue regeneration. *Adv Food Nutr Res* 2014; 73: 59–81.
28. Klokkevold PR, Vandemark L, Kenney EB, Bernard GW. Osteogenesis enhanced by chitosan (poly-N-acetyl glucosaminoglycan) in vitro. *J Periodontol* 1996; 67: 1170–1175.
29. Ho MH, Yao CJ, Liao MH, Lin PI, Liu SH, Chen RM. Chitosan nanofiber scaffold improves bone healing via stimulating trabecular bone production due to upregulation of the Runx2/osteocalcin/alkaline phosphatase signaling pathway. *Int J Nanomedicine* 2015; 10: 5941–5954.
30. Levengood SL, Zhang M. Chitosan-based scaffolds for bone tissue engineering. *J Mater Chem B Mater Biol Med* 2014; 2: 3161–3184.
31. Oryan A, Sahviah S. Effectiveness of chitosan scaffold in skin, bone and cartilage healing. *Int J Biol Macromol* 2017; 104: 1003–1011.
32. Yang Y, Rossi FM, Putnins EE. Periodontal regeneration using engineered bone marrow mesenchymal stromal cells. *Biomaterials.* 2010; 31(33): 8574-8582.

33. Zang S, Jin L, Kang S, Hu X, Wang M, Wang J, Chen B, Peng B, Wang Q. Periodontal Wound Healing by Transplantation of Jaw Bone Marrow-Derived Mesenchymal Stem Cells in Chitosan/Anorganic Bovine Bone Carrier Into One- Wall Infrabony Defects in Beagles. *J Periodontol.* 2016; 87(8): 971-981.
34. Lemaitre M, Monsarrat P, Blasco-Baque V, Loubières P, Burcelin R, Casteilla L, Planat-Bénard V, Kémoun P. Periodontal Tissue Regeneration Using Syngeneic Adipose-Derived Stromal Cells in a Mouse Model. *Stem Cells Transl Med.* 2017; 6(2): 656-665.
35. Hung CN, Mar K, Chang HC, Chiang YL, Hu HY, Lai CC, Chu RM, Ma CM. A comparison between adipose tissue and dental pulp as sources of MSCs for tooth regeneration. *Biomaterials.* 2011; 32(29): 6995-7005.
36. Walmsley GG, Senarath-Yapa K, Wearda TL, Menon S, Hu MS, Duscher D, Maan ZN, Tsai JM, Zielins ER, Weissman IL, Gurtner GC, Lorenz HP, Longaker MT. Surveillance of Stem Cell Fate and Function: A System for Assessing Cell Survival and Collagen Expression In Situ. *Tissue Eng Part A.* 2016;22(1-2) :31- 40.
37. Prati C, Zamparini F, Botticelli D, Ferri M, Yonezawa D, Piattelli A, Gandolfi MG. The Use of ESEM-EDX as an Innovative Tool to Analyze the Mineral Structure of Peri-Implant Human Bone. *Materials (Basel).* 2020; 13(7): 1671.
38. Feng X. Chemical and Biochemical Basis of Cell-Bone Matrix Interaction in Health and Disease. *Curr Chem Biol.* 2009;3(2):189-196.
39. Kourkoumelis N, Balatsoukas I, Tzaphlidou M. Ca/P concentration ratio at different sites of normal and osteoporotic rabbit bones evaluated by Auger and energy dispersive X-ray spectroscopy. *J Biol Phys.* 2012; 38(2): 279-291.
40. Kumar, G. S. *Orban's oral histology & embryology.* Elsevier Health Sciences; 2011.
41. Rowe P, Koller A, Sharma S. *Physiology, bone remodeling.* StatsPearls. Treasure Island; 2018.
42. Zimmermann B, Wachtel HC, Noppe C. Patterns of mineralization in vitro. *Cell Tissue Res.* 1991; 263(3): 483-93.
43. Roodman GD. Regulation of osteoclast differentiation. *Ann N Y Acad Sci.* 2006; 1068:100-109.
44. Nanci A: *Ten Cate's Oral Histology: Development, Structure, and Function,* 7th ed. Mosby; 2005.
45. Raggatt LJ, Partridge NC. Cellular and molecular mechanisms of bone remodeling. *J Biol Chem.* 2010; 285(33): 25103-25108.
46. Liu H, Yazici H, Ergun C, Webster TJ, Bermek H. An in vitro evaluation of the Ca/P ratio for the cytocompatibility of nano-to-micron particulate calcium phosphates for bone regeneration. *Acta Biomater.* 2008 Sep;4(5):1472-9.
47. Allen, M. R., & Burr, D. B. Bone Growth, Modeling, and Remodeling. In *Basic and Applied Bone Biology.* academic Press; 2019: 85-100.
48. Mellis DJ, Itzstein C, Helfrich MH, Crockett JC. The skeleton: a multi-functional complex organ: the role of key signalling pathways in osteoclast differentiation and in bone resorption. *J Endocrinol.* 2011; 211(2): 131-43.
49. Morgan EF, Barnes GL, Einhorn TA. In: *Osteoporosis.* Marcus R, Feldman D, Nelson DA, Rosen CJ. San Diego: Academic Press; 2008: 3–26.
50. Boskey AL. Bone composition: relationship to bone fragility and antiosteoporotic drug effects. *Bonekey Rep.* 2013; 2: 447.
51. Zhu W, Robey PG, Boskey AL. In: *Osteoporosis.* Marcus R, Feldman D, Nelson DA, Rosen CJ. San Diego: Academic Press; 2008: 191–240.
52. Halcrow SE, Rooney J, Beavan N, Gordon KC, Tayles N, Gray A (2014) Assessing Raman Spectroscopy as a Prescreening Tool for the Selection of Archaeological Bone for Stable Isotopic Analysis. *PLoS ONE* 9(7): e98462.
53. Okata H, Nakamura M, Henmi A, Yamaguchi S, Mikami Y, Shimauchi H, Sasano Y. Calcification during bone healing in a standardised rat calvarial defect assessed by micro-CT and SEM-EDX. *Oral Dis.* 201; 21(1): 74-82.
54. Henmi A, Okata H, Mikami Y, Sasano Y. Calcification in rat developing mandibular bone demonstrated by whole mount staining, microcomputed tomography and scanning electron microscopy with energy dispersive X-ray spectroscopy. *Biomed Res.* 2017; 38(5): 277-284.
55. Bellahcène A, Castronovo V, Ogbureke KU, Fisher LW, Fedarko NS. Small integrin-binding ligand N-linked glycoproteins (SIBLINGs): multifunctional proteins in cancer. *Nat Rev Cancer.* 2008; 8(3): 212-226.

56. Fisher LW, Torchia DA, Fohr B, Young MF, Fedarko NS. Flexible structures of SIBLING proteins, bone sialoprotein, and osteopontin. *Biochem Biophys Res Commun.* 2001; 280(2): 460-465.
57. Baht GS, Hunter GK, Goldberg HA. Bone sialoprotein-collagen interaction promotes hydroxyapatite nucleation. *Matrix Biol.* 2008; 27(7): 600-608.
58. Gordon JA, Tye CE, Sampaio AV, Underhill TM, Hunter GK, Goldberg HA. Bone sialoprotein expression enhances osteoblast differentiation and matrix mineralization in vitro. *Bone.* 2007; 41(3):462-473.
59. Singh A, Gill G, Kaur H, Amhmed M, Jakhu H. Role of osteopontin in bone remodeling and orthodontic tooth movement: a review. *Prog Orthod.* 2018; 19(1): 18.
60. Goretti Penido M, Alon US. Phosphate homeostasis and its role in bone health. *Pediatr Nephrol.* 2012; 27(11): 2039-2048.



ASDJ

Ain Shams Dental Journal